BIOCHEMISTRY
including biophysical chemistry & molecular biology

Article

pubs.acs.org/biochemistry

Structural Role of Compensatory Amino Acid Replacements in the α-Synuclein Protein

Valeria Losasso,[†,‡] Adriana Pietropaolo,[§] Claudio Zannoni,[∥] Stefano Gustincich,*[,†] and Paolo Carloni*[,‡]

[†]International School for Advanced Studies (SISSA), 34136 Trieste, Italy

[‡]German Research School for Simulation Sciences, FZ-Jülich and RWTH Aachen, Wilhelm-Johnen-Strasse, 52428 Jülich, Germany

[§]Università di Catanzaro, Dipartimento di Scienze Farmacobiologiche, 88100 Catanzaro, Italy

[∥]Università di Bologna, Dipartimento di Chimica Fisica ed Inorganica, 40136 Bologna, Italy

Supporting Information

ABSTRACT: A subset of familial Parkinson's disease (PD) cases is associated with the presence of disease-causing point mutations in human α-synuclein [huAS(wt)], including A53T. Surprisingly, the human neurotoxic amino acid 53T is present in non-primate, wild-type sequences of α-synucleins, including that expressed by mice [mAS(wt)]. Because huAS(A53T) causes neurodegeneration when expressed in rodents, the amino acid changes between the wild-type human protein [huAS(wt)] and mAS(wt) might act as intramolecular suppressors of A53T toxicity in the mouse protein, restoring its physiological structure and function. The lack of structural information for mAS(wt) in aqueous solution has prompted us to conduct a comparative molecular dynamics study of huAS(wt), huAS(A53T), and mAS(wt) in water at 300 K. The calculations are based on an ensemble of nuclear magnetic resonance-derived huAS(wt) structures. huAS(A53T) turns out to be more flexible and less compact than huAS(wt). Its central (NAC) region, involved in fibril formation by the protein, is more solvent-exposed than that of the wild-type protein, in agreement with nuclear magnetic resonance data. The compactness of mAS(wt) is similar to that of the human protein. In addition, its NAC region is less solvent-exposed and more rigid than that of huAS(A53T). All of these features may be caused by an increase in the level of intramolecular interactions on passing from huAS(A53T) to mAS(wt). We conclude that the presence of "compensatory replacements" in the mouse protein causes a significant change in the protein relative to huAS(A53T), restoring features not too dissimilar to those of the human protein.

Parkinson's disease (PD) is a neurodegenerative disease affecting ∼5 million people worldwide.[1] In post-mortem brains of sporadic PD patients, proteinaceous fibrillar aggregates, called Lewy bodies, represent the neuropathological hallmark of the disease. The major components of Lewy bodies are fibrils of human α-synuclein [huAS(wt)][2] whose function has not been fully elucidated.[3]

huAS(wt) exists both in cytosol and bound to the membrane.[4] While it assumes a partially helical conformation in micelles,[5] NMR,[6−8] electron and fluorescence microscopy,[9] and circular dichroism (CD)[10−12] showed that huAS(wt) is a naturally unfolded protein in aqueous solution (Figure 1b) where it may establish long-range interactions. In vitro and in vivo, huAS(wt) fibrillates, forming a heterogeneous set of amyloid-like filaments and oligomers that are intimately involved in pathogenesis.[10,13]

huAS(wt) features three domains (Figure 1a). The N-terminal (amino acids 1−60) amphipathic domain contains four 11-residue imperfect repeats. The hydrophobic domain of residues 61−95 contains two additional repeats and the amyloidogenic NAC (non-amyloid component) region. Hydrophobic residues 71−82 of this region are involved in the conversion into fibrillar species.[14,15] Indeed, fluorimetry, electron microscopy, immunoelectron microscopy, and circular dichroism spectroscopy[15−18] have shown that these residues are crucial for fibril formation. In addition, deletion of residues 76 and 77 strongly impairs aggregation.[18]

The SNCA gene encoding AS[19] has been found mutated in rare familial cases of PD. Together with pathological duplications, three point mutations, A30P,[20] E46K,[21] and A53T,[22] have been identified. Interestingly, the latter two fibrillate in vitro faster than huAS(wt),[23,24] while huAS(A30P) fibrillates slower.[23] In the resulting fibrils, the C-terminal domain of huAS(A53T) is more compact than that of huAS(wt), as revealed by solid-state NMR spectroscopy as well as electron and atomic force microscopy.[23,25,26]

A30P and E46K mutations involve conserved amino acids across all species as expected for a disease-provoking mutation (Figure S1 of the Supporting Information). Instead, A53 is not evolutionarily conserved.[22] Intriguingly, in non-primate mammals, A is replaced by T, which is the familial mutation in PD. 53T is accompanied by as many as six other substitutions in mouse and rat, and seven in horse. Because huAS(A53T) causes neurodegeneration when expressed in rodents,[19,27−32]

Received: May 16, 2011
Revised: July 5, 2011
Published: July 8, 2011

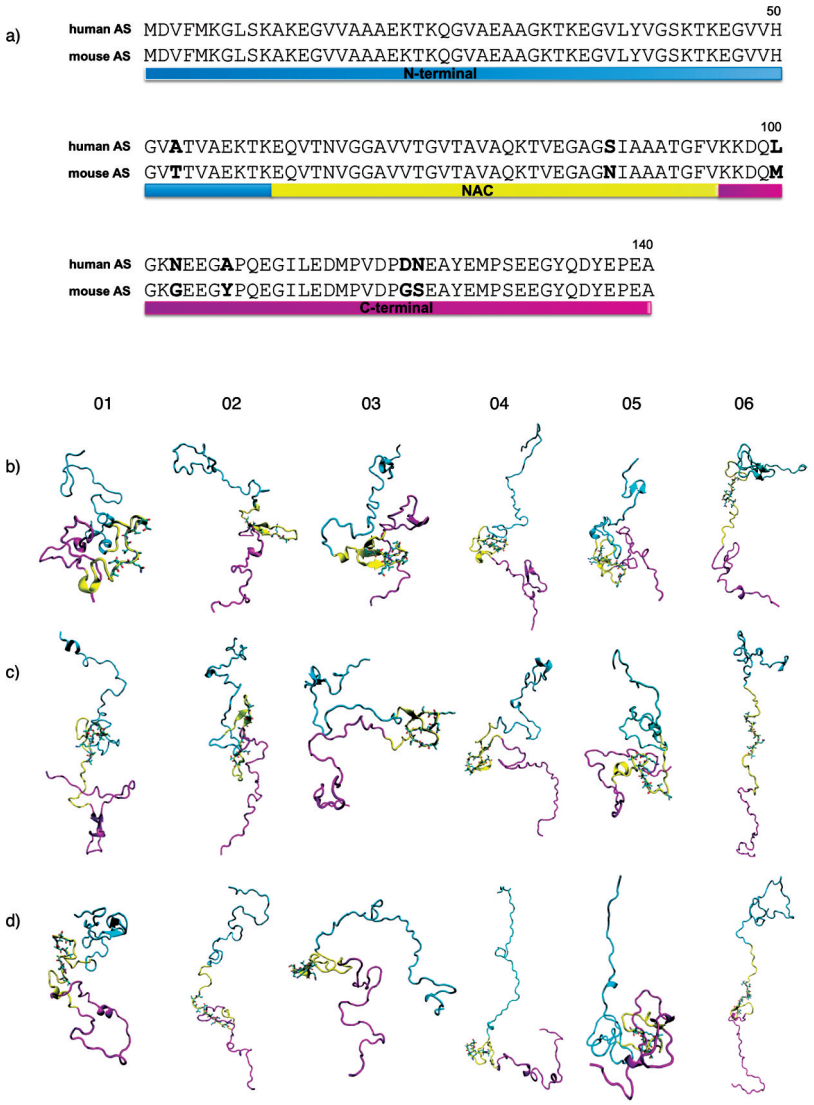

Figure 1. (a) Sequence alignment between huAS(wt) and mAS(wt). The residues changing from one species to another are highlighted in bold. The alignment has been obtained using ClustalW (http://www.ebi.ac.uk/clustalw). (b–d) Backbone representations of the six selected MD structures (01–06) of huAS(wt) (b), huAS(A53T) (c), and mAS(wt) (d), obtained via the computational procedure outlined in the text. The side chains of residues 71–82 are also displayed.

some of the additional substitutions [S87N, L100M, N103G, A107Y, D121G, and N122S (see Figure 1a)] might have a compensatory effect on A53T, restoring its physiological behavior. Such behavior might arise from several factors. These might include changes of post-translation modifications, such as the loss of phosphorylation at position 87[33] caused by the S87N mutation. Indeed, S87 phosphorylation occurs in vivo within Lewy bodies. The level is increased in brains of transgenic (TG) models of synucleinopathies and human post-mortem brains from several neurodegenerative diseases but not from normal controls.[33] This compensatory behavior could also arise, at least in part, from changes in the structural features of the protein. These changes are the focus of these studies.

So far, biophysical methods have provided important insights into the differences between the wild-type protein and the A53T variants.

A53T causes a detachment in the NAC region in the phospholipid-bound form, which then becomes solvent-exposed.[34] Furthermore, it causes an overall increase in the level of extended structure in aqueous solution relative to that of the wild-type protein.[35] As observed by NMR,[36] FRET,[37] and SMF[38] experiments, long-range interactions present in huAS(wt) are lost. Finally, the overall flexibility of the protein increases.[36] It is thus clear[a] that A53T affects huAS(wt) structure and plasticity both in solution and when bound to the phospholipids.[35,36] Therefore, one might expect that "compensatory" changes in the mouse α-synuclein [mAS(wt)] primary sequence restore the physiological structure and plasticity of huAS(wt) in the presence of 53T. Unfortunately, the lack of structural information about mAS(wt) in water solution and/or anchored to the membrane[b] has so far not answered the key question: does mAS(wt) share structural determinants with huAS(wt) while differing significantly from the disease-linked variant?

To explore the structural role of the compensatory amino acid changes in mice, we perform a comparative submicrosecond molecular dynamics (MD) simulation study with huAS(wt), huAS(A53T), and mAS(wt). We focus on the protein in aqueous solution because the detailed NMR-derived structures of huAS(wt) have been determined.[6,8] These are

dx.doi.org/10.1021/bi2007564 | *Biochemistry* 2011, 50, 6994–7001

here used as a starting point for this work. The study is conducted therefore in aqueous solution at 300 K. It covers overall a submicrosecond time scale and takes advantage of the so-called chirality index analysis. This allows detection of secondary structure motifs and protein backbone flexibility, as shown already for the prion protein.[43,44]

We first investigate the structural determinants of huAS(wt) and huAS(A53T) proving that our calculations based on the Amber99SB force field reproduce the experimental structural information obtained by SMF and NMR. We then take advantage of the same computational protocol to identify the structure and conformational fluctuations of mAS(wt) unveiling the role of the compensatory amino acid substitutions from human to the mouse protein to suppress the neurotoxic effect of the A53T mutation (Figure 1a).

METHODS

We clustered the huAS(wt) ensemble obtained by NMR data using the algorithm from ref 45 with a cutoff of 22 Å. This cutoff corresponds to the maximum of the Gaussian-like shape of the C_α rmsd (root-mean-square distance) distribution, calculated over each pair combination of conformations. In this way, we obtained 23 clusters. The first six of them, covering 73% of the conformations, were selected. The former have populations of 0.4, 0.12, 0.07, 0.06, 0.04, and 0.04, respectively. Six huAS(A53T) conformers were constructed by replacing A53 with T and, in the case of mAS(wt), also S87 with N, L100 with M, N103 with G, A107 with Y, D121 with G, and N122 with S, in the six representatives of huAS(wt). Swiss-PdbViewer was used.[46] The 18 systems were inserted into a water box. The size of the water box was chosen so that there was a minimum distance of 10 Å between any atom and the edge of the box. The number of added water molecules varied largely (between ~25000 and ~60000), according to the compactness of the structure. Nine, nine, and eight Na^+ counterions were added to neutralize the huAS(wt), huAS(A53T), and mAS(wt) systems, respectively.

The AMBER ff99SB,[47] Aaqvist,[48] and TIP3P[49] force fields were used for the protein, sodium ions, and water, respectively. Periodic boundary conditions were applied. Electrostatic interactions were calculated using the particle mesh Ewald method.[50] The time step was set to 2 fs. The SHAKE algorithm[51] was applied to fix all bond lengths. A cutoff distance of 10 Å was used for electrostatic and van der Waals interactions. Room conditions (T = 300 K, and P = 1.013 bar) were achieved by coupling the systems with a Langevin thermostat[52] with a coupling coefficient of 5 ps, and a Nosé-Hoover Langevin barostat[53] with an oscillation period of 200 fs and a damping time scale of 100 fs; 40 ns of MD for each of the six clusters was conducted for huAS(wt), huAS(A53T), and mAS(wt) for a total of 0.72 μs using NAMD version 2.7.[54]

Several properties were calculated with the equilibrated MD structures (see the Supporting Information for details): (i) the normalized average $C_\alpha-C_\alpha$ contact maps, (ii) the normalized aromatic stacking maps, defined in terms of Y/F rings' centers of mass distances and the angle formed by the two vectors along the C_2 axis of the F/Y benzyl moieties, (iii) salt bridges, which are assumed to exist if the distance between the R-NH_3^+ groups of lysines and the R-COO^- groups of glutamates and aspartates is less than 3.5 Å, (iv) the average gyration radius, which is calculated as described in ref 55, and (v) the CD spectrum, which is calculated using the DichroCalc program suite[56] considering the semiempirical parameters of ref 57. It is averaged according to the population of huAS(wt) representative clusters.[58] It is reported for all the representative clusters in huAS(A53T) and mAS because for the latter the contribution of each representative to the contribution of the ensemble of structures of the proteins is not known, in contrast to that of huAS(wt). (vi) The intensity ratios for huAS(wt) are the ratios of cross-peak intensities in the spectra of the oxidized and reduced states of the spin-label as a function of residue number. They have been measured for selected cysteine mutants, namely, residues 24, 42, 62, 87, and 103. These were calculated using the formula of ref 59. (vii) The solvent exposure of the NAC domain in terms of the solvent accessible surface area (SASA) was calculated as described in ref 60. (viii) The backbone local flexibility content is calculated on the basis of the so-called chirality index per residue (G) and its standard deviations (σG).[43,61,62] An increase in σG indicates an increase in flexibility.[44] (ix) The normalized correlation functions for pairs of residues undergoing substitutions involve different residues or the same residue, e.g., A53T/S87N or A53T/A53T. They were calculated as a function of time on the basis of the chirality indices. As usual, full correlation occurs when the function is equal to 1. A decrease in this value points to a decreased correlation. From those, we obtain the $1/t$ quantity defined in Results.

RESULTS

Six representatives [01−06 (Figure 1b)] of huAS(wt) NMR structures were investigated with MD simulations based on the Amber99SB force field.[47] These representatives were extracted by cluster analysis[45] from the ensemble of 4000 structures revealed by NMR spectroscopy.[8] They represent 73% of the conformations. They have been previously used to investigate the binding of dopamine and dopamine derivatives to huAS(wt).[63,64] Overall, calculations are conducted for 0.24 μs. As shown in Table 1, the calculated average gyration radii for 01−06 were 25, 28, 27, 38, 21, and 43 Å, respectively. These are similar to those of initial NMR structures (Table 1).

Table 1. Gyration Radii (angstroms) for the Six MD Ensembles of huAS(wt), huAS(A53T), and mAS(wt)[a]

structure	huAS(wt)	huAS(A53T)	mAS(wt)	NMR structure
01	24.8 (7.4)	31.7 (2.8)	26.1 (5.0)	39.4
02	28.0 (4.1)	32.6 (1.6)	36.9 (2.3)	35.1
03	27.5 (3.9)	32.4 (2.9)	28.1 (4.0)	35.6
04	38.3 (5.0)	41.3 (6.8)	43.3 (2.7)	46.0
05	21.2 (2.4)	21.4 (3.0)	23.1 (3.4)	29.6
06	42.6 (5.3)	59.0 (2.5)	52.7 (4.0)	53.3

[a]Standard deviations are given in parentheses. The initial NMR values for huAS(wt) are also reported.

Contact maps are presented in Figure 2a. These results are consistent with NMR data that identified compact and unordered conformations with average gyration radii of 24.7 and 41.9 Å, respectively.[6,8]

According to our calculations, conformers are classified in three classes (Figure 1c). One class, derived from conformers 1 and 5, includes conformations with long-range packing. The second class, derived from conformers 2, 4, and 6, is random coil. The last class, derived from conformer 3, features β-like structures. The presence of these classes is fully consistent with

dx.doi.org/10.1021/bi2007564 | Biochemistry 2011, 50, 6994−7001

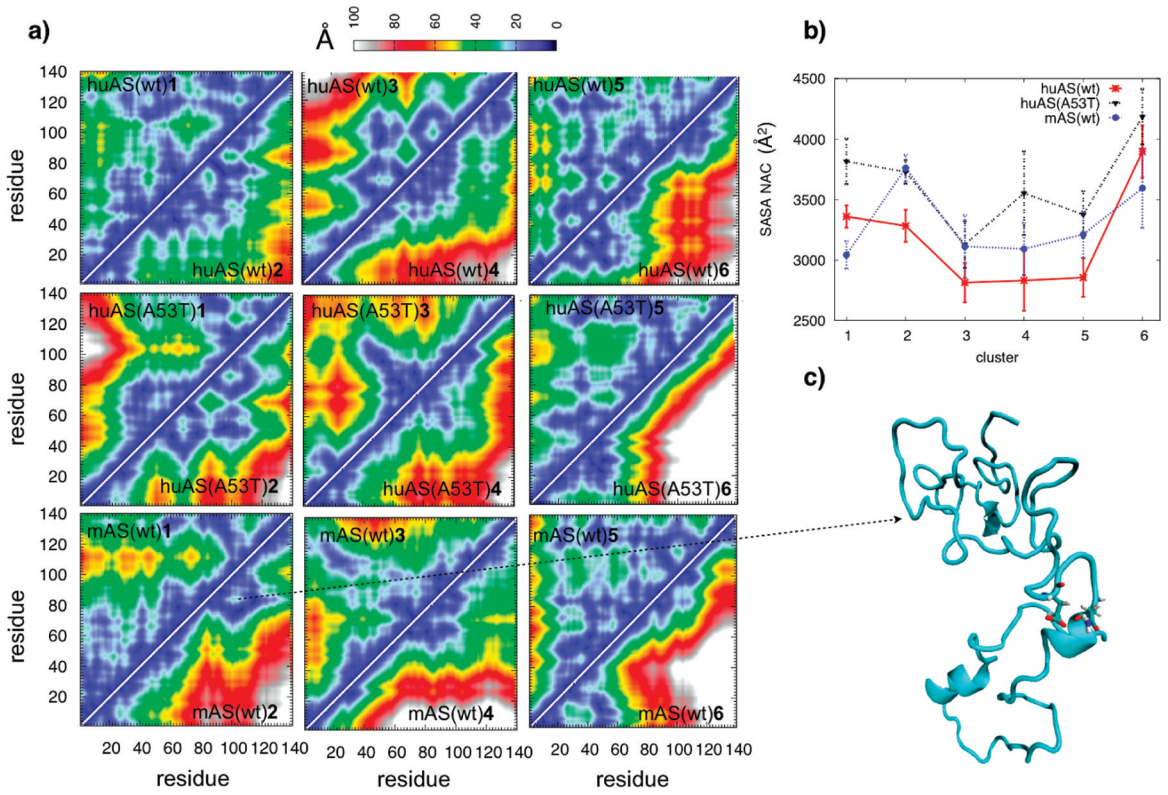

Figure 2. (a) Contact maps of huAS(wt), huAS(A53T), and mAS(wt) representatives. Long-range contacts are present only in huAS(wt)1 and huAS(wt)5 (the number from 1 to 6 indicates the extent of cluster population, 1 being the most populated cluster). Few extents of long-range contacts are present in mAS(wt)1, mAS(wt)5, and huAS(A53T)5. The standard deviations of the values in the contact maps are reported in Figure S6 of the Supporting Information. (b) Solvent accessible surface area (SASA) for the NAC region of huAS(wt), huAS(A53T), and mAS(wt).

evidence from single-molecule force spectroscopy (SMF) experiments.[65]

Contact maps identified N-terminal−C-terminal and NAC−C-terminal long-range interactions. Contacts were present for residues 60−80 with 120−140, as well as for the domain of residues 80−90 with the region of residues 120−140 (Figure 2a). This result is consistent with NMR data[6,8] as well as with OPLS-based MD simulations starting from the completely stretched structure of the protein.[66]

The calculated CD spectrum (Figure S2 of the Supporting Information) reproduces the one obtained experimentally.[11,12] It indicates a high level of random coil structure.

The "intensity ratios"[8,59] are the ratios of cross-peak intensities in the spectra of the oxidized and reduced states of the spin-label. These ratios, calculated for each residue of the protein, are in fairly good agreement with the experimental data[8] (see the legend of Figure S3 of the Supporting Information for more details).

We next compare our computational predictions on huAS(wt) with those on huAS(A53T). For this purpose, we took advantage of available SMF and NMR experimental data for the human mutant protein.

First, the N-terminal−C-terminal and NAC−C-terminal long-range interactions present in huAS(A53T) are lost. The average gyration radii of most conformers are larger than the corresponding radii in huAS(wt), pointing to an overall decrease in compactness (Table 1). This is also observed by visual inspection of the structure (Figure 1b). These results are consistent with NMR data, which showed the absence of long-range contacts in huAS(A53T) and the presence of a rather extended structure.[35,36] These findings are also consistent with SMF experiments, which demonstrated that huAS(A53T) exhibits a limited mechanical resistance to unfolding.[38] Interestingly, the calculated solvent accessible surface area (SASA) of the NAC region is larger than in huAS(wt) (Figure 2b). This finding is also consistent with NMR data.[36] Finally, the overall flexibility of the mutant (especially in its NAC region) is larger than that of huAS(wt), as shown by the calculation of the standard deviation of the chirality index [σG in Figure 3 (see the Supporting Information for details)] and by NMR data.[36] In our calculations, the increase in SASA and the flexibility of the NAC region in huAS(A53T) are caused by the loss of NAC−C-terminal interactions (Figure 2b) that shield the NAC region of huAS(wt) and render it more rigid.

We thus conclude that our simulation protocol reproduces all known structure and conformational properties of huAS(wt) and huAS(A53T).

We then apply the same computational setup to analyze mAS(wt). This features the A53T along with the S87N, L100M, N103G, A107Y, D121G, and N122S substitutions.

As shown in Figure 2c, mAS(wt) adopts two separately packed domains, the N- and C-terminal cores. As a result, the compactness of the structure is not too dissimilar from that of huAS(wt), as shown by the calculation of the gyration radii (Table 1) and the contact maps (Figure 2a). The C-terminal and, more strongly, the N-terminal cores are stabilized by intradomain salt bridges (Table S2 of the Supporting

dx.doi.org/10.1021/bi2007564 | Biochemistry 2011, 50, 6994−7001

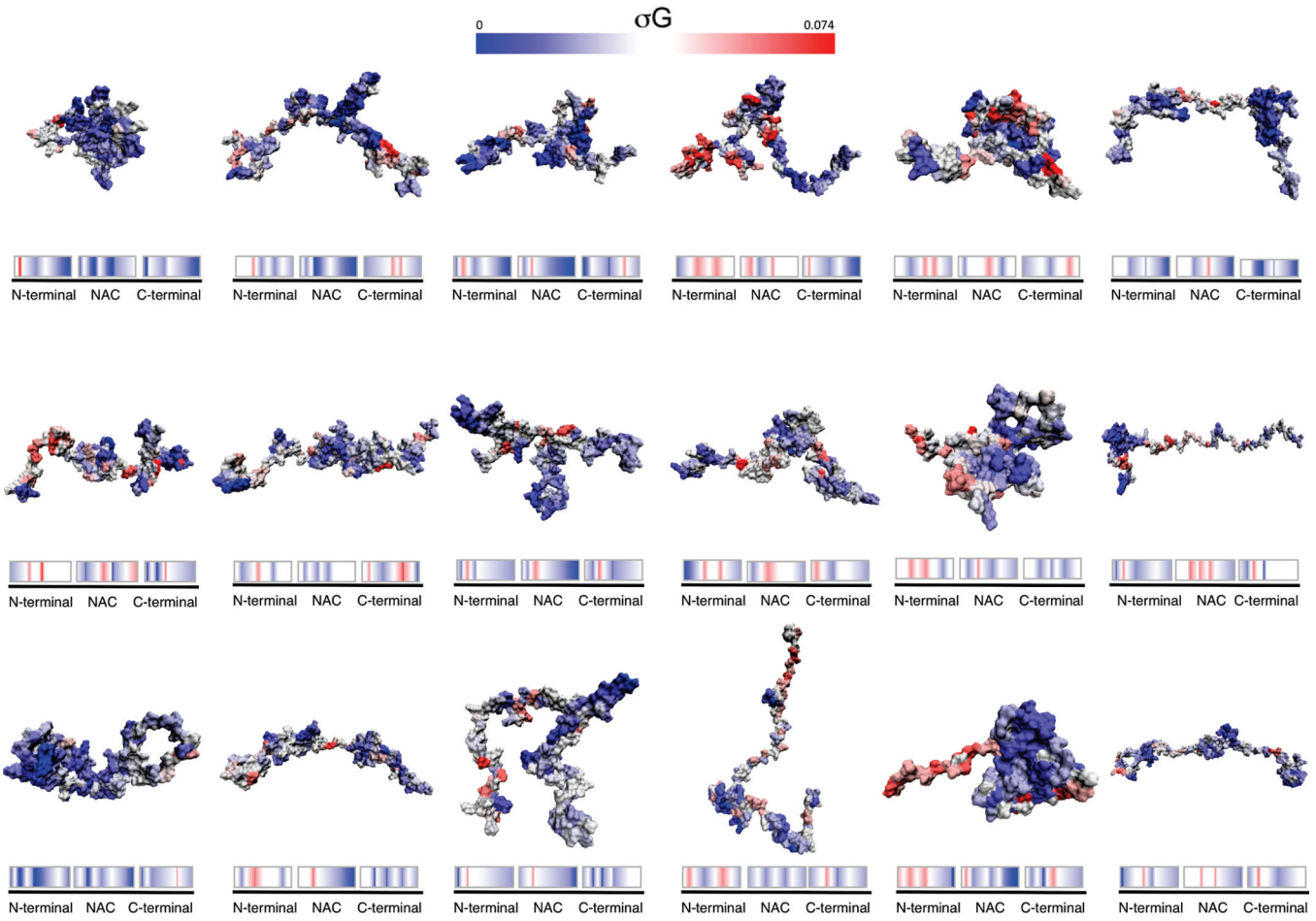

Figure 3. Snapshots for the six MD ensembles of huAS(wt), huAS(A53T), and mAS(wt). The structures are colored according to their degree of flexibility. Structures are oriented with the N-termini on the left and the C-termini on the right.

Information). The SASA of the NAC region is smaller than that of huAS(A53T) (Figure 2b).

Interestingly, the flexibility of mAS(wt) (and in particular of the NAC region) is comparable to that of huAS(wt) and lower than that of huAS(A53T) (Figure 3). The lower flexibility of the C-terminus relative to huAS(A53T) is likely to be caused by intramolecular interactions that are not present in huAS(A53T) (Figure 2a). These include (i) the π-stacking interactions between the aromatic rings of Y133 and Y136 (Figure S4 of the Supporting Information) and (ii) the N87−E83 H-bond, which extends from the NAC region to the upstream region of the C-terminal domain (Figure 2a).

Insights into the flexibility of the residues undergoing substitutions are obtained from an analysis of the correlation functions among the backbone atoms of these residues. These functions represent the correlation between the instantaneous chirality of different residues. Figure S5 of the Supporting Information shows an example of those. Constant values of such correlations indicate low relative flexibility (see Methods). Within a certain time scale τ, this function will vary by 100% of its initial value. We may say then that the original correlation is then practically lost. We therefore use the reciprocal of this quantity $(1/\tau)$ as another index for flexibility that can change the local chirality (Table 2). The $1/\tau$ values turn out to be larger for the disease-linked variant than those of the other two proteins. This points to a higher flexibility of the residue undergoing substitutions in huAS(A53T). A consistent picture is obtained by analyzing the flexibility indices previously defined in terms of standard deviations of chirality indices (Tables S3−S5 of the Supporting Information). Furthermore, the residues being substituted in the C-termini of huAS(wt) and huAS(A53T) are more flexible than those of mAS(wt). The chirality index analysis also provides consistent results in this case (Tables S3−S5 of the Supporting Information).

DISCUSSION

The dominant huAS(A53T) mutation is responsible for a subset of familial cases of PD. The structural features of this protein have been extensively studied to improve our understanding of the structural bases of neurotoxicity. In this context, NMR data as well as SMF experiments have provided important descriptions of differences and commonalities with huAS(wt). Surprisingly, while the overexpression of huAS(A53T) in mouse may induce neurodegeneration, mAS(wt) presents an A53T substitution, similar to the pathogenic mutation in humans. It was therefore important to study the role of the six additional amino acid changes between mouse and human primary sequences on mAS(wt) structure to identify potential intramolecolar suppressors of A53T toxicity.

Unfortunately, the lack of structural information about mAS(wt) in water solution and/or anchored to the membrane has so far hampered our ability to address it in this study.

Here we report a computational protocol that accurately predicts structural and plasticity properties for huAS(wt) and

dx.doi.org/10.1021/bi2007564 | *Biochemistry* 2011, 50, 6994−7001

Table 2. $1/\tau$ Values (ns^{-1}) for huAS(wt) Structures (left values), huAS(A53T) Structures (center values), and mAS(wt) Structures (right values)[a]

residues	structure 01			structure 02			structure 03			structure 04			structure 05			structure 06		
53−53	0	0.2	0	0	0	0	0	0.2	0	0	0	0	0	0.1	0	0	0	0
53−87	0	0.2	0.1	0.1	0.1	0	0	0	0	0.7	0.2	0.1	0	0	0.1	0	1	1
53−100	0	0	0.1	0	0.2	0	0	0	0.1	0.1	0.2	0	0	0.2	0	0.7	0	0
53−103	0	0	1	0	0	1	0.2	0.2	0.1	0.2	0.3	0	0	0.5	0	0.1	0	0
53−107	0	1	0.2	0.1	0.1	0	0	0	0	0.1	0.1	0.2	0.1	0.1	0	0	0	0
53−121	0	0.1	0	0.5	0.1	0	0	0.2	0.1	0	0	0.1	0	0	0	0	0.2	0.2
53−122	0	0.1	0	0.2	0.1	0	0.5	0.1	0	0	0.1	0	0	0.1	0	0	0.5	0.5
87−87	0	0	0.5	0	1	0.1	0	0	0	0	0.1	0	0	0	0.1	0	1	0.5
87−100	0	0.1	0.1	1	0.1	0	0	0	0	0	0.1	0.1	0	0.1	0	0	1	1
87−103	0	0.1	1	1	1	0.1	0.2	0.1	0.1	0.1	0.1	0.5	0.1	0.1	0	0.1	0.5	0.5
87−107	0	1	0.2	0.3	0.1	0	0.1	0	0	0	0.1	1	0.1	0	0	0.1	0.5	0.5
87−121	0	0.3	0.1	0.1	0.2	0	0	0	0.1	0	0.1	0.2	0.1	0	0	0.1	0.5	0.5
87−122	0	1	0	0	1	0	0.1	0.1	0	0	0.1	0.2	0.1	0.2	0	0.1	1	1
100−100	0	0	1	0	0.2	0	0	0	1	0.1	0.2	0	0.1	0	0	0.1	0	0
100−103	0	0	0.1	0	0.2	0.1	0.2	0	0.1	0.1	0.1	0	0.1	0.1	0.1	0	0	0
100−107	0	1	0.1	0.1	0.2	0	0	0	0	0	1	0.3	0.1	0	0	0	0	0
100−121	0	0	0.1	1	1	0	0	0	0.1	0	1	0	0.1	0	0	0	0.1	0.1
100−122	0	0.2	0.1	1	0.1	0	0.2	1	0	0	0.5	0	1	0.1	0	0	0.2	0.2
103−103	0	0	0.5	0.1	0	0.5	0.1	0	0.1	0.5	0.3	0.1	0	0.3	0	0	1	0
103−107	0	1	1	0.2	1	0.1	0.1	0.1	0.1	0	0.1	0.2	0.1	0.3	0	0	0	0
103−121	0	0	0	0.3	0.1	0.1	0.1	0.1	0.1	0.1	0.1	0	0	0.3	0.1	0.1	0.2	0.2
103−122	0	0.1	0	0.5	0.1	0.3	0.3	0.2	0.1	0.1	1	0.1	0.1	1	0	0.1	0.1	0.1
107−107	0	0.2	0	0	0.1	0	0	0	0	0	0.2	0.3	0.1	0	0	0	0	0
107−121	0	0.1	0	0	0.1	0	0	0	0	0	0	0.1	0.1	0	0.1	0	0.2	0.2
107−122	0	0	0	0.1	1	0	0.1	0.1	0	0	0.1	0.5	0.2	0.1	0	0	0.1	0.1
121−121	0	0	0	0.1	0	0	0	0	0.1	0	0	0	0	0	0	0	0.2	0.2
121−122	0	0.1	0	0	0	0	0.1	0.1	0	0	0.1	0	0.1	1	0	0	0.2	0.2
122−122	0	0.2	0	0.2	0.2	0	0.1	0.1	0	0	0.1	0	0.1	0.1	0	0	0.2	0.2

[a]Values corresponding to $1/\tau$ values longer than the MD time window are set to 0.

huAS(A53T) recapitulating NMR and SMF experimental data. For this purpose, we take advantage of the chirality index.[43,44]

We then use this computational setup to predict the structure and flexibility of mAS(wt).

Our calculations show that the presence of compensatory amino acid substitutions in mAS(wt) does restore key structural aspects of huAS(wt). In particular, a variety of intramolecular interactions allow the NAC region of mAS(wt) to be significantly more compact and less flexible than in huAS(A53T). In this context, the formation of the N87−E83 H-bond, which extends from the NAC region to the upstream region of the C-terminal domain (Figure 2a), is especially relevant. Indeed, S87 in huAS(wt) and in huAS(A53T) does not form this H-bond with E83 or any other residues of the protein.

It is also interesting to note that E83 was previously shown to be essential in the ability of dopamine to inhibit huAS(wt) fibril formation.[63] We conclude that the presence of compensatory replacements in the mouse protein causes a rather dramatic change in the structure and plasticity of the protein, restoring structural features not too dissimilar from those of huAS(wt). Future experiments in vivo and in vitro should address the role of S87N substitution as an intramolecular suppressor of A53T toxicity.

■ ASSOCIATED CONTENT

Supporting Information

Methods, supplemental tables, and figures. This material is available free of charge via the Internet at http://pubs.acs.org.

■ AUTHOR INFORMATION

Corresponding Author

*S.G.: telephone, +39-040-3787-705; fax, +39-040-3787-702; e-mail, gustinci@sissa.it. P.C.: telephone, +49-2461-61-8941; fax, +49-2461-61-8942; e-mail, p.carloni@grs-sim.de.

Author Contributions

V.L. and A.P. contributed equally to this work.

Notes

[a]MD studies of the protein in micelles point to a lower degree of flexibility of huAS(A53T) with respect to that of huAS(wt).[39] MD studies of the protein in a lipid bilayer also provide interesting insights into the wild-type structures, suggesting in particular that the truncated protein (residues 1−95) forms a bent helix because of its collective motions,[40] and that the truncated fragment (residues 31−52) assumes a high degree of conformational disorder.[41]

[b]NMR has provided insights into the protein in the solid state at 263 K.[42] mAS(wt) was found to lose transient C-terminal−NAC contacts and C-terminal−N-terminal contacts. The N-terminal domain was more rigid and the NAC region more solvent exposed relative to those of huAS(wt).

■ ACKNOWLEDGMENTS

We thank Michele Vendruscolo for providing them with the 4000 NMR structures of huAS(wt).

■ ABBREVIATIONS

PD, Parkinson's disease; huAS(wt), human wild-type α-synuclein; huAS(A53T), human α-synuclein carrying the A53T mutation; mAS(wt), mouse α-synuclein; NMR, nuclear magnetic resonance; NAC, non-amyloid component region; CD, circular dichroism; FRET, fluorescence resonance energy transfer; SMF, single-molecule force spectroscopy; MD, molecular dynamics; SASA, solvent accessible surface area.

■ REFERENCES

(1) Shehadeh, L. A., Yu, K., Wang, L., Guevara, A., Singer, C., Vance, J., and Papapetropoulos, S. (2010) SRRM2, a potential blood biomarker revealing high alternative splicing in Parkinson's disease. *PLoS One 5*, e9104.

(2) Spillantini, M. G., Schmidt, M. L., Lee, V. M., Trojanowski, J. Q., Jakes, R., and Goedert, M. (1997) α-Synuclein in Lewy bodies. *Nature 388*, 839−840.

(3) Bonini, N. M., and Giasson, B. I. (2005) Snaring the function of α-synuclein. *Cell 123*, 359−361.

(4) Lee, H. J., Choi, C., and Lee, S. J. (2002) Membrane-bound α-synuclein has a high aggregation propensity and the ability to seed the aggregation of the cytosolic form. *J. Biol. Chem. 277*, 671−678.

(5) Ulmer, T. S., and Bax, A. (2005) Comparison of structure and dynamics of micelle-bound human α-synuclein and Parkinson disease variants. *J. Biol. Chem. 280*, 43179−43187.

(6) Bertoncini, C. W., Jung, Y. S., Fernández, C. O., Hoyer, W., Griesinger, C., Jovin, T. M., and Zweckstetter, M. (2005) Release of long-range tertiary interactions potentiates aggregation of natively unstructured α-synuclein. *Proc. Natl. Acad. Sci. U.S.A. 102*, 1430−1435.

(7) Rasia, R. M., Bertoncini, C. W., Marsh, D., Hoyer, W., Cherny, D., Zweckstetter, M., Griesinger, C., Jovin, T. M., and Fernández, C. O. (2005) Structural characterization of copper(II) binding to α-synuclein: Insights into the bioinorganic chemistry of Parkinson's disease. *Proc. Natl. Acad. Sci. U.S.A. 102*, 4294−4299.

(8) Dedmon, M. M., Lindorff-Larsen, K., Christodoulou, J., Vendruscolo, M., and Dobson, C. M. (2005) Mapping long-range interactions in α-synuclein using spin-label and ensemble molecular dynamics simulations. *J. Am. Chem. Soc. 127*, 476−477.

(9) Hoyer, W., Cherny, D., Subramaniam, V., and Jovin, T. M. (2004) Impact of the acidic C-terminal region comprising amino acids 109−140 on α-synuclein aggregation in vitro. *Biochemistry 43*, 16233−16242.

(10) Hong, D. P., Xiong, W., Chang, J. Y., and Jiang, C. (2011) The role of the C-terminus of human α-synuclein: Intra-disulfide bonds between the C-terminus and other regions stabilize non-fibrillar monomeric isomers. *FEBS Lett. 585*, 561−566.

(11) Eliezer, D., Kutluay, E., Bussell, R., and Browne, G. (2001) Conformational properties of α-synuclein in its free and lipid-associated states. *J. Mol. Biol. 307*, 1961−1973.

(12) Maiti, N. C., Apetri, M. M., Zagorski, M. H., Carey, P. R., and Anderson, V. E. (2004) Raman spectroscopic characterization of secondary structure in natively unfolded protein: α-Synuclein. *J. Am. Chem. Soc. 126*, 2399−2408.

(13) Murray, I. V. J., Giasson, B. I., Quinn, S. M., Koppaka, V., Axelsen, P. H., Ischiropoulos, H., Trojanowsky, J. Q., and Lee, V. M. (2003) Role of α-synuclein carboxy-terminus on fibril formation in vitro. *Biochemistry 42*, 8530−8540.

(14) Bodles, A.M., Guthrie, D. J., Greer, B., and Irvine, G. B. (2001) Identification of the region of non-Aβ component (NAC) of Alzheimer's disease amyloid responsible for its aggregation and toxicity. *J. Neurochem. 78*, 384−395.

(15) Giasson, B. I., Murray, I. V., Trojanowski, J. Q., and Lee, V. M. (2001) A hydrophobic stretch of 12 amino acid residues in the middle of α-synuclein is essential for filament assembly. *J. Biol. Chem. 276*, 2380−2386.

(16) Der Sarkissian, A., Jao, C. C., Chen, J., and Langen, R. (2003) Structural organization of α-synuclein fibrils studied by site-directed spin labeling. *J. Biol. Chem. 278*, 37530−37535.

(17) Del Mar, C., Greenbaum, E. A., Mayne, L., Englander, S. W., and Woods, V. L. (2005) Structure and properties of α-synuclein and other amyloids determined at the amino acid level. *Proc. Natl. Acad. Sci. U.S.A. 102*, 15477−15482.

(18) Waxman, E. A., Mazzulli, J. R., and Giasson, B. I. (2009) Characterization of hydrophobic residue requirements for α-synuclein fibrillization. *Biochemistry 48*, 9427−9436.

(19) Shulman, J. M., De Jager, P. L., and Feany, M. B. (2011) Parkinson's disease: Genetics and pathogenesis. *Annu. Rev. Pathol. 6*, 193−222.

(20) Kruger, R., Kuhn, W., Muller, T., Woitalla, D., Graeber, M., Kösel, S., Przuntek, H., Epplen, J. T., Schöls, L., and Riess, O. (1998) Ala30Pro mutation in the gene encoding α-synuclein in Parkinson's disease. *Nat. Genet. 18*, 106−108.

(21) Zarranz, J. J., Alegre, J., Gomez-Esteban, J. C., Lezcano, E., Ros, R., Ampuero, I., Vidal, L., Hoenicka, J., Rodriguez, O., Atares, B., Llorens, V., Gomez Tortosa, E., del Ser, T., Munoz, D. G., and de Yebenes, J. G. (2004) The new mutation, E46K, of α-synuclein causes Parkinson and Lewy-body dementia. *Ann. Neurol. 55*, 164−173.

(22) Polymeropoulos, M. H., Lavedan, C., Leroy, E., Ide, S. E., Dehejia, A., Dutra, A., Pike, B., Root, H., Rubenstein, J., Boyer, R., Stenroos, E. S., Chandrasekharappa, S., Athanassiadou, A., Papapetropoulos, T., Johnson, W. G., Lazzarini, A. M., Duvoisin, R. C., Di Iorio, G., Golbe, L. I., and Nussbaum, R. L. (1997) Mutation in the α-synuclein gene identified in families with Parkinson's disease. *Science 276*, 2045−2047.

(23) Conway, K. A., Harper, J. D., and Lansbury, P. T. (1998) Accelerated in vitro fibril formation by a mutant α-synuclein linked to early-onset Parkinson disease. *Nat. Med. 4*, 1318−1320.

(24) Fredenburg, R. A., Rospigliosi, C., Meray, R. K., Kessler, J. C., Lashuel, H. A., Eliezer, D., and Lansbury, P. T. (2007) The impact of the E46K mutation on the properties of α-synuclein in its monomeric and oligomeric states. *Biochemistry 46*, 7107−1118.

(25) Heise, H., Celej, M. S., Becker, S., Riedel, D., Pelah, A., Kumar, A., Jovin, T. M., and Baldus, M. (2003) Solid-state NMR reveals structural differences between fibrils of wild-type and disease-related A53T mutant α-synuclein. *J. Mol. Biol. 380*, 444−450.

(26) Suk, J. E., Lokappa, S. B., and Ulmer, T. S. (2010) The clustering and spatial arrangement of β-sheet sequence, but not order, govern α-synuclein fibrillogenesis. *Biochemistry 49*, 1533−1540.

(27) Graham, D. R., and Sidhu, A. (2010) Mice expressing the A53T mutant form of human α-synuclein exhibit hyperactivity and reduced anxiety-like behavior. *J. Neurosci. Res. 88*, 1777−1783.

(28) Giasson, B. I., Duda, J. E., Quinn, S. M., Zhang, B., Trojanowski, J. Q., and Lee, V. M. (2002) Neuronal α-synucleinopathy with severe movement disorder in mice expressing A53T human α-synuclein. *Neuron 34*, 521−533.

(29) Koprich, J. B., Johnston, T. H., Reyes, M. G., Sun, X., and Brotchie, J. M. (2010) Expression of human A53T α-synuclein in the rat substantia nigra using a novel AAV1/2 vector produces a rapidly evolving pathology with protein aggregation, dystrophic neurite architecture and nigrostriatal degeneration with potential to model the pathology of Parkinson's disease. *Mol. Neurodegener. 5*, 43.

(30) Tsika, E., Moysidou, M., Guo, J., Cushman, M., Gannon, P., Sandaltzopoulos, R., Giasson, B. I., Krainc, D., Ischiropoulos, H., and Mazzulli, J. R. (2010) Distinct region-specific α-synuclein oligomers in A53T transgenic mice: Implications for neurodegeneration. *J. Neurosci. 30*, 3409−3418.

(31) Gispert, S., Del Turco, D., Garrett, L., Chen, A., Bernard, D. J., Hamm-Clement, J., Korf, H. W., Deller, T., Braak, H., Auburger, G., and Nussbaum, R. L. (2003) Transgenic mice expressing mutant A53T human α-synuclein show neuronal dysfunction in the absence of aggregate formation. *Mol. Cell. Neurosci. 24*, 419−429.

(32) Kurz, A., Double, K. L., Lastres-Becker, I., Tozzi, A., Tantucci, M., Bockhart, V., Bonin, M., García-Arencibia, M., Nuber, S., Schlaudraff, F., Liss, B., Fernández-Ruiz, J., Gerlach, M., Wüllner, U., Lüddens, H., Calabresi, P., Auburger, G., and Gispert, S. (2010) A53T-α-synuclein overexpression impairs dopamine signaling and striatal synaptic plasticity in old mice. *PLoS One 5*, e11464.

(33) Paleologou, K. E., Oueslati, A., Shakked, G., Rospigliosi, C. C., Kim, H. Y., Lamberto, G. R., Fernández, C. O., Schmid, A., Chegini, F., Gai, W. P., Chiappe, D., Moniatte, M., Schneider, B. L., Aebischer, P., Eliezer, D., Zweckstetter, M., Masliah, E., and Lashuel, H. A. (2010) Phosphorylation at S87 is enhanced in synucleinopathies, inhibits α-synuclein oligomerization, and influences synuclein-membrane interactions. *J. Neurosci. 30*, 3184−3198.

(34) Bodner, C. R., Maltsev, A. S., Dobson, C. M., and Bax, A. (2010) Differential phospholipid binding of AS variants implicated in Parkinson's disease revealed by solution NMR spectroscopy. *Biochemistry 49*, 862−871.

(35) Bussell, R., and Eliezer, D. (2001) Residual structure and dynamics in Parkinson's disease-associated mutants of α-synuclein. *J. Biol. Chem. 276*, 45996−46003.

(36) Bertoncini, C. W., Fernández, C. O., Griesinger, C., Jovin, T. M., and Zweckstetter, M. (2005) Familial mutants of α-synuclein with increased neurotoxicity have a destabilized conformation. *J. Biol. Chem. 280*, 30649−30652.

(37) Lee, J. C., Langen, R., Hummel, P. A., Gray, H. B., and Winkler, J. R. (2004) α-Synuclein structures from fluorescence energy-transfer kinetics: Implications for the role of the protein in Parkinson's disease. *Proc. Natl. Acad. Sci. U.S.A. 101*, 16466−16471.

(38) Brucale, M., Sandal, M., Di Maio, S., Rampioni, A., Tessari, I., Tosatto, L., Bisaglia, M., Bubacco, L., and Samorì, B. (2009) Pathogenic mutations shift the equilibria of α-synuclein single molecules towards structured conformers. *ChemBioChem 10*, 176−183.

(39) Perlmutter, J. D., Braun, A., and Sachs, J. N. (2009) Curvature dynamics of α-synuclein familial Parkinson disease mutants: Molecular simulations of the micelle- and bilayer-bound forms. *J. Biol. Chem. 284*, 7177−7189.

(40) Mihajlovic, M., and Lazaridis, T. (2008) Membrane-bound structure and energetics of α-synuclein. *Proteins 70*, 761−768.

(41) Bortolus, M., Tombolato, F., Tessari, I., Bisaglia, M., Mammi, S., Bubacco, L., Ferrarini, A., and Maniero, A. L. (2008) Broken helix in vesicle and micelle-bound α-synuclein: Insights from site-directed spin labeling-EPR experiments and MD simulations. *J. Am. Chem. Soc. 130*, 6690−6691.

(42) Wu, K. P., Kim, S., Fela, D. A., and Baum, J. (2008) Characterization of conformational and dynamic properties of natively unfolded human and mouse α-synuclein ensembles by NMR: Implications for aggregation. *J. Mol. Biol. 378*, 1104−1115.

(43) Pietropaolo, A., Muccioli, L., Berardi, R., and Zannoni, C. (2008) A chirality index for investigating protein secondary structures and their time evolution. *Proteins 70*, 667−677.

(44) Pietropaolo, A., Muccioli, L., Zannoni, C., and Rizzarelli, E. (2009) Conformational preferences of the full chicken prion protein in solution and its differences with respect to mammals. *ChemPhysChem 10*, 1500−1510.

(45) Micheletti, C., Seno, F., and Maritan, A. (2000) Recurrent oligomers in proteins: An optimal scheme reconciling accurate and concise backbone representations in automated folding and design studies. *Proteins 40*, 662−674.

(46) Guex, N., and Peitsch, M. C. (1997) SWISS-MODEL and the Swiss-PdbViewer: An environment for comparative protein modeling. *Electrophoresis 18*, 2714−2723.

(47) Hornak, V., Abel, R., Okur, A., Strockbine, B., Roitberg, A., and Simmerling, C. (2006) Comparison of multiple Amber force fields and development of improved protein backbone parameters. *Proteins 65*, 712−725.

(48) Aaqvist, J. (1990) Ion-water interaction potentials derived from free energy perturbation simulations. *J. Phys. Chem. 94*, 8021−8024.

(49) Jorgensen, W. L., Chandrasekhar, J., Madura, J. D., Impey, R. W., and Klein, M. L. (1983) Comparison of simple potential functions for simulating liquid water. *J. Chem. Phys. 79*, 926−935.

(50) Darden, T., York, D., and Pedersen, L. (1993) Particle mesh Ewald: An N-log(N) method for Ewald sums in large systems. *J. Chem. Phys. 98*, 10089−10093.

(51) Ryckaert, J.P., Ciccotti, G., and Berendsen, H. J. C. (1977) Numerical integration of the Cartesian equations of motion of a system with constraints: Molecular dynamics of n-alkanes. *J. Comput. Phys. 23*, 327−341.

(52) Adelman, S. A., and Doll, J. D. (1976) Generalized Langevin equation approach for atom/solid surface scattering: General formulation for classical scattering off harmonic solids. *J. Chem. Phys. 64*, 2375−2388.

(53) Feller, S. E., Zhang, Y., Pastor, R. W., and Brooks, B. R. (1995) Constant pressure molecular dynamics simulation: The Langevin piston method. *J. Chem. Phys. 103*, 4613−4621.

(54) Phylips, J. C., Braun, R., Wang, W., Gumbart, J., Tajkhorshid, E., Villa, E., Chipot, C., Skeel, R. D., Kalé, L., and Schulten, K. (2005) Scalable molecular dynamics with NAMD. *J. Comput. Chem. 26*, 1781−1802.

(55) Humphrey, W., Dalke, A., and Schulten, K. (1996) VMD: Visual molecular dynamics. *J. Mol. Graphics 14*, 33−38.

(56) Bulheller, B. M., and Hirst, J. D. (2009) DichroCalc: Circular and linear dichroism online. *Bioinformatics 25*, 539−540.

(57) Sreerama, N., and Woody, R. W. (2000) Estimation of protein secondary structure from circular dichroism spectra: Comparison of CONTIN, SELCON, and CDSSTR methods with an expanded reference set. *Anal. Biochem. 287*, 252−260.

(58) Glättli, A., Daura, X., Seebach, D., and van Gunsteren, W. F. (2002) Can one derive the conformational preference of a β-peptide from its CD spectrum? *J. Am. Chem. Soc. 124*, 12972−12978.

(59) Teilum, K., Kragelund, B. B., and Poulsen, F. M. (2002) Transient structure formation in unfolded acyl-coenzyme A-binding protein observed by site-directed spin labelling. *J. Mol. Biol. 324*, 349−357.

(60) Futamura, N., Aluru, S., Ranjan, D., and Hariharan, B. (2002) Efficient parallel algorithms for solvent accessible surface area of proteins. *IEEE Transactions on Parallel Distributed Systems 13*, 544−555.

(61) Osipov, M. A., Pickup, B. T., and Dunmur, D. A. (1995) A new twist to molecular chirality: intrinsic chirality indices. *Mol. Phys. 84*, 1193−1206.

(62) Solymosi, M., Low, R. J., Grayson, M., and Neal, M. P. (2002) A generalized scaling of a chiral index for molecules. *J. Chem. Phys. 116*, 9875−9881.

(63) Herrera, F. E., Chesi, A., Paleologou, K. E., Schmid, A., Munoz, A., Vendruscolo, M., Vendruscolo, M., Gustincich, S., Lashuel, H. A., and Carloni, P. (2008) Inhibition of α-synuclein fibrillization by dopamine is mediated by interactions with five C-terminal residues and with E83 in the NAC region. *PLoS One 3*, e3394.

(64) Latawiec, D., Herrera, F. E., Bek, A., Losasso, V., Candotti, M., Benetti, F., Carlino, E., Kranjc, A., Lazzarino, M., Gustincich, S., Carloni, P., and Legname, G. (2010) Modulation of α-synuclein aggregation by dopamine analogs. *PLoS One 5*, e9234.

(65) Sandal, M., Valle, F., Tessari, I., Mammi, S., Bergantino, E., Musiani, F., Brucale, M., Bubacco, L., and Samorì, B. (2008) Conformational equilibria in monomeric α-synuclein at the single-molecule level. *PLoS Biol. 6*, 99−108.

(66) Wu, K. P., Weinstock, D. S., Narayanan, C., Levy, R. M., and Baum, J. B. (2009) Structural reorganization of α-synuclein at low pH observed by NMR and REMD simulations. *J. Mol. Biol. 391*, 784−796.